INSTITUTE OF PHYSICS PUBLISHING NANOTECHNOLOGY
Nanotechnology **17** (2006) 1574–1579 doi:10.1088/0957-4484/17/6/007

Atomic force microscopy with inherent disturbance suppression for nanostructure imaging

A W Sparks[1] **and S R Manalis**[1,2,3]

[1] Biological Engineering Division, Massachusetts Institute of Technology, Cambridge, MA 02139, USA
[2] Department of Mechanical Engineering, Massachusetts Institute of Technology, Cambridge, MA 02139, USA

E-mail: scottm@media.mit.edu

Received 2 December 2005, in final form 16 January 2006
Published 21 February 2006
Online at stacks.iop.org/Nano/17/1574

Abstract
Scanning probe imaging is often limited by disturbances, or mechanical noise, from the environment that couple into the microscope. We demonstrate, on a modified commercial atomic force microscope, that adding an interferometer as a secondary sensor to measure the separation between the base of the cantilever and the sample during conventional feedback scanning can result in real-time images with inherently suppressed out-of-plane disturbances. The modified microscope has the ability to resolve nanometre-scale features in situations where out-of-plane disturbances are comparable to, or even several orders of magnitude greater than, the scale of the topography. We present images of DNA in air from this microscope in tapping mode without vibration isolation, and show improved clarity using the interferometer as the imaging signal. The inherent disturbance suppression approach is applicable to all scanning probe imaging techniques.

(Some figures in this article are in colour only in the electronic version)

1. Introduction

Scanning probe microscopes (SPMs) are unique in their ability to offer sub-ångström resolution in ambient imaging environments. Unfortunately, they are highly sensitive to disturbances, or mechanical noise, that couple into the microscope and affect the tip–sample interaction. These disturbances, which include vibrations of various microscope components, drift of the piezo scanner, and thermal expansion of the microscope, are worse in an ambient environment due to high thermal energy at room temperature and the permeability of the air or fluid medium to sound. The common solutions to this problem are: the use of a rigid microscope, which can limit sample size and versatility; vibration isolation, which can be costly and difficult to optimize for a particular microscope environment; and image filtering, which requires a knowledge of the spectral distribution of both the topography and the dominant noise sources.

[3] Author to whom any correspondence should be addressed.

The cause of this problem is that the actuator, whose input is used to construct the image, must compensate for both the scanned topography and the disturbances in order to control the tip–sample interaction. Despite the use of feedback, a scanning probe microscope cannot distinguish between the topography of the imaged sample and the effects of disturbances. A few groups have addressed this problem for specific imaging modes [1, 2], but the only known solution that is independent of the scanning mode was demonstrated by Schitter and Stemmer [3]. In their work, a capacitive sensor was attached to the SPM to measure disturbances, which were scaled and subtracted from the image offline. However, this approach required manual compensation and did not compensate for the entire mechanical path of the microscope. Disturbances affecting the piezo scanner, in particular, could not be measured.

We recently introduced a new approach, referred to as inherent disturbance suppression, capable of addressing this problem [4]. It requires the use of a secondary sensor,

mounted adjacent to the scanning probe, that measures the separation between the probe and the average sample height. This sensor accounts for the entire mechanical path of the microscope and averages the sample topography over an area much larger than the tip. With the probe sensor output held constant by the feedback loop, the secondary sensor output reveals mostly topography with disturbances suppressed significantly. We demonstrated this technique [4] for scanning tunnelling microscopy (STM) by integrating a tunnelling tip on a micromachined cantilever with an interferometer, which averages the sample height over an area determined by the spot size of a focused laser. However, the STM implementation could not be extended to atomic force microscopy (AFM) due to the requirement of a non-compliant cantilever. It was also limited by the need for a custom-fabricated device and a home-made microscope to incorporate the optical readout hardware of the interferometer. In addition, because the tunnelling tip and interferometer were only 30 μm apart, the sample was constrained to optically flat substrates so as not to diffract the interferometer laser.

In this paper, we show how inherent disturbance suppression can be extended to any SPM imaging or spectroscopy mode on any sample, and we demonstrate its effectiveness using tapping mode AFM, the most widely used mode, to image single DNA molecules. This technique is implemented using a standard cantilever and commercial SPM, which is minimally modified to accommodate the interferometer.

2. The inherent disturbance suppression technique

The principles that explain inherent disturbance suppression are illustrated in figure 1. We refer to the out-of-plane direction as Z and any direction in the sample plane as XY. In this figure, the scanning probe is visualized as mounted adjacent to an interferometer [5, 6] such that the base of the scanning probe and the interferometer can be treated as a single rigid body. In the case of AFM, the scanning probe detects force and is designed to deflect in response to the sample topography at the tip. The output of this 'localized' sensor is input to a feedback loop that controls a Z actuator to hold the tip–sample force constant. Images are constructed simultaneously from the voltage input of the actuator, as in a traditional SPM, and the 'delocalized' interferometer output, which measures the separation between the scanning probe base and the average sample height. In figure 1(a), we consider the effect of scanning the sample in XY for an ideal SPM free from disturbances. As the tip is scanned in XY from the peak to the valley of a topographic feature, the feedback corrects the Z actuator voltage to maintain a fixed tip–sample force. The interferometer, which for an optically flat sample would not detect the XY scanning motion without Z feedback, measures a change in average sample height δ due to the actuator correction. Thus, both actuator and interferometer measure topography. In figure 1(b), we consider the inverse case where there is no XY scanning, but the probe is displaced in Z by a disturbance δ. The feedback again compensates to maintain a constant force, but because the probe and sample are displaced equally, the average separation does not change. Only the actuator signal carries the disturbance signature.

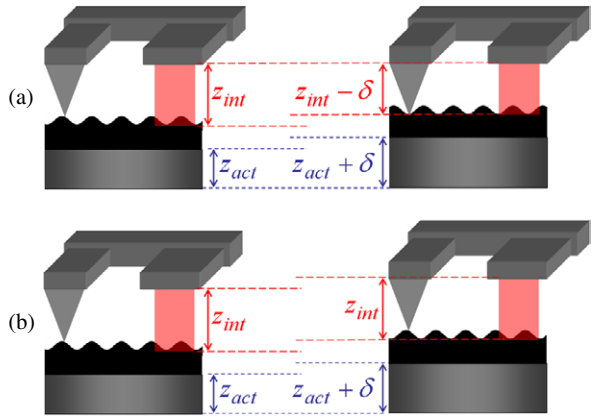

Figure 1. The inherent disturbance suppression concept, as generalized for contact AFM. The 'localized' scanning probe sensor holds the cantilever deflection constant in feedback by adjusting the relative displacement z_{act} of a piezoelectric actuator. An interferometer is used as the 'delocalized' sensor and measures the separation z_{int}. In (a), the sample is scanned laterally in the absence of disturbances, while in (b), the probe is displaced vertically in the absence of lateral scanning.

Superposing these two cases, the actuator, as conventionally observed, responds to both topography and disturbances, while the interferometer measures only the topography.

Figure 1 is completely independent of the imaging mode: the scanning probe can be a flexible cantilever, as in contact AFM, or a rigid one, as in STM. It is essential only that the tip–sample interaction does not affect the interferometer, except due to the reaction of the Z actuator to the feedback signal. Furthermore, any sensor that measures separation over a sample area larger than the image scan could replace the interferometer as the 'delocalized' sensor. A capacitive sensor would be particularly suitable, although it would require a conductive sample or sample mount.

The inherent disturbance suppression phenomenon can be understood analytically using a Laplace-domain block diagram model, as shown in figure 2. In this diagram, four transfer functions are defined: $C(s)$, the feedback controller; $A(s)$, the Z actuator; $S_{\mathrm{probe}}(s)$, the scanning probe Z sensor; and $S_{\mathrm{int}}(s)$, the interferometer. For simplicity, the linearized dynamics of the cantilever and tip–sample interaction can be lumped with the actuator transfer function for frequencies within the feedback bandwidth. The Z actuator input voltage, $v_{\mathrm{act}}(s)$, and the interferometer output voltage, $v_{\mathrm{int}}(s)$, are used to generate the sample images. There are also four external signals to consider, all of which are displacements: $t_Z(s)$, the topography of the sample; $d_Z(s)$, out-of-plane disturbances; $n_{\mathrm{probe}}(s)$, the noise from the scanning probe sensor; and $n_{\mathrm{int}}(s)$, the interferometer noise. The placement of these signals in the diagram is justified by considering the effect of turning the feedback off: the scanning probe sensor output will reflect topography, disturbances, and its inherent sensor noise, while the interferometer signal will consist of only disturbances and its sensor noise. The loop function, $L(s)$, is defined as the product of the transfer functions in the feedback loop:

$$L(s) \equiv C(s)A(s)S_{\mathrm{probe}}(s). \tag{1}$$

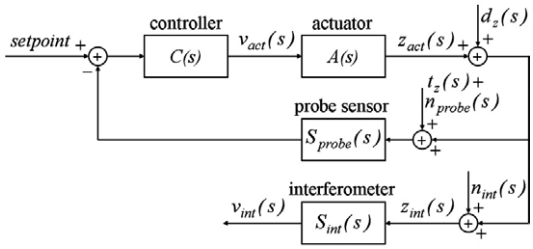

Figure 2. Block diagram model for the two-sensor SPM with relevant noise sources.

Using superposition, the imaging signals can be predicted as a function of the topography and noise sources:

$$V_{\mathrm{act}}(s) = (t_Z(s) + n_{\mathrm{probe}}(s) + d_Z(s))\frac{C(s)S_{\mathrm{probe}}(s)}{1 + L(s)} \tag{2}$$

$$V_{\mathrm{int}}(s) = S_{\mathrm{int}}(s)\Bigg((t_Z(s) + n_{\mathrm{probe}}(s))\frac{L(s)}{1 + L(s)} + d_Z(s)\frac{1}{1 + L(s)} + n_{\mathrm{int}}(s)\Bigg). \tag{3}$$

For frequencies below the cut-off of the feedback loop, $A(s)$ and $S_{\mathrm{int}}(s)$ can be assumed constant, allowing the imaging signals to be written as displacements $z_{\mathrm{act}}(s)$ and $z_{\mathrm{int}}(s)$:

$$z_{\mathrm{act}}(s) = (t_Z(s) + n_{\mathrm{probe}}(s) + d_Z(s))\frac{L(s)}{1 + L(s)} \tag{4}$$

$$z_{\mathrm{int}}(s) = (t_Z(s) + n_{\mathrm{probe}}(s))\frac{L(s)}{1 + L(s)} + d_Z(s)\frac{1}{1 + L(s)} + n_{\mathrm{int}}(s). \tag{5}$$

Assuming $L(s) \gg 1$ within the feedback bandwidth:

$$z_{\mathrm{act}}(s) = t_Z(s) + n_{\mathrm{probe}}(s) + d_Z(s) \tag{6}$$

$$z_{\mathrm{int}}(s) = t_Z(s) + n_{\mathrm{probe}}(s) + \frac{d_Z(s)}{L(s)} + n_{\mathrm{int}}(s). \tag{7}$$

It is apparent that the actuator signal reveals topography, but cannot suppress either disturbances or the noise from the scanning probe sensor. The interferometer signal reveals topography and probe sensor noise but suppresses disturbances. However, this comes at the expense of added noise from the interferometer. Accordingly, for this technique to improve image quality, three criteria must be satisfied:

(1) the image must be adversely affected by Z disturbances;
(2) the disturbance frequencies must be within the feedback bandwidth; and
(3) the interferometer noise must be small compared to the Z disturbances.

The second condition is satisfied on most AFMs, which typically have feedback bandwidths of around 1 kHz and disturbances below 100 Hz. The third condition has been satisfied on both a home-made [4] and the commercial SPM described in this work, although the noise of the interferometer could be reduced further.

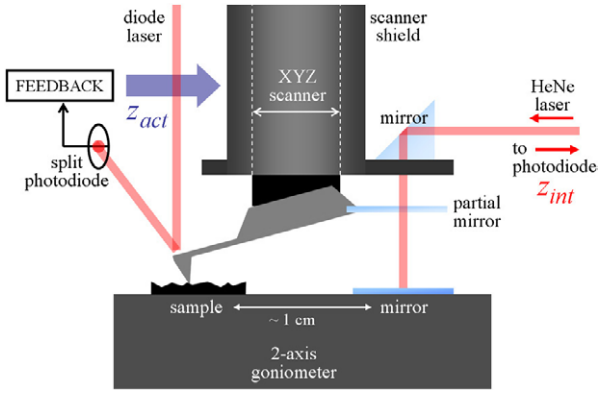

Figure 3. Modified commercial AFM incorporating interferometer readout optics and a 2-axis goniometer for angular adjustment. The right-angle mirror is fixed to the scanner shield and does not move during scanning.

3. Implementation on a commercial SPM

The disturbance suppression technique has been implemented on a commercial SPM, the Dimension 3000 (Veeco Instruments, USA). This microscope is capable of imaging a 6-inch wafer; alternatively, its head, which integrates the piezo scanner and optical lever hardware, can be mounted on an inverted optical microscope for simultaneous fluorescence measurements. As a result of this versatility, it has a longer mechanical path and is more susceptible to disturbances than a smaller SPM. The microscope was modified to accommodate an interferometer, as shown in figure 3. A simple Fabry–Perot interferometer was adequate for this application, and consisted of a 0.15 mm thick glass slide fragment metallized with 10 nm gold, which was used as a low-reflectance mirror, and a piece of silicon metallized with 4 nm titanium and 40 nm gold, used as a high-reflectance mirror. The low-reflectance mirror was mounted to the AFM tip holder with wax, while the high-reflectance mirror was magnetically mounted to a 2-axis goniometer, which ensured the two mirrors were parallel. The angular adjustment is critical to maximizing the sensitivity of the interferometer. Also mounted to the goniometer magnet was the sample, which was located 1–2 cm from the mirror. Although this distance is great compared to our previous implementation [4], we still observe a high degree of coherence between the two sensors.

A HeNe laser (1125, JDS Uniphase, USA) was used for the interferometer readout. Due to the 5 mm pathlength difference of this interferometer, a diode laser was not sufficiently coherent to produce a strong readout signal. The laser was directed parallel to the sample and reflected off a metallized right-angle prism in a downward direction to the interferometer. The prism was mounted to the concentric cylindrical steel shield surrounding the piezo scanner and, therefore, remained fixed during scanning. The interfering beam reflections were redirected along the same path, and separated from the incident beam by a beamsplitter (not shown). A photodiode (DET110, Thorlabs, USA) detected the intensity of the reflected signal, which was then buffered and input to the microscope controller (Nanoscope IIIa, Veeco) via a signal access module. To minimize the effects of convection

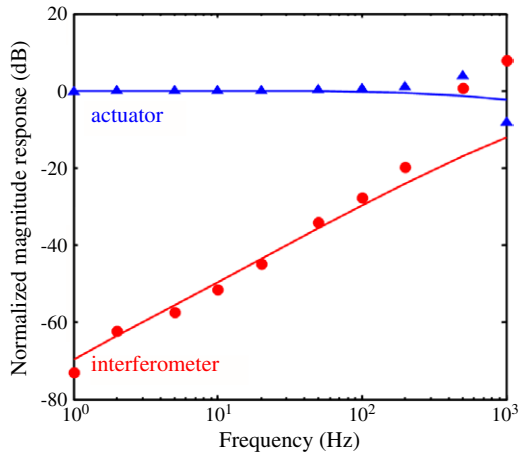

Figure 4. Response of the actuator and interferometer signals to synthesized sinusoidal Z disturbances. The curves are fit to the data points based on first-order control theory.

and hum on the noise of the sensors, the microscope was enclosed in a dark, conductive box, but was not otherwise isolated from vibrations. The noise floor of the microscope in this environment, which was dominated by Z disturbances, was measured to be 0.5 nm rms in a 0.1 Hz–1 kHz bandwidth. The interferometer noise is estimated from our previous work [4, 6] to be, at most, 0.1 nm rms in this bandwidth. It is probably limited by laser intensity noise and optical pathlength noise induced by thermal and refractive index variations in the cavity.

In this work, we present data using tapping mode AFM imaging [7] in air using commercial silicon probes (TESP, Veeco) with optical lever detection. Our emphasis on tapping mode results from its importance in virtually eliminating lateral shear forces during imaging, allowing adsorbed biological structures to be imaged noninvasively. Furthermore, tapping mode is characterized by smaller average normal forces than contact mode, allowing the probe tip to remain sharp after repeated imaging. Tapping mode uniquely relies on both contact and non-contact effects, and its successful implementation with disturbance suppression demonstrates the universality of this approach to any SPM imaging mode.

3.1. Disturbance response measurement—tapping mode AFM

To test the disturbance suppression ability of the microscope, the Z actuator was modulated with large amplitude (>10 nm) sinusoids intended to mimic real Z disturbances. The rms values of both the actuator and interferometer signals were measured simultaneously by lock-in amplifiers from 1 Hz to 1 kHz, and are shown in figure 4. The controller design determines the suppression performance as it can be assumed to dominate the frequency response of the loop gain $L(s)$ at frequencies within the feedback bandwidth. Pure integral control was selected to eliminate dc error in the force on the tip and ensure stable and robust operation.

In figure 4, the lock-in measurements are presented along with curves predicting the suppression performance for a simplified system with $L(s) = 20\,000/s$. As expected from (4), the actuator response is independent of $L(s)$ until close to the feedback bandwidth, 3 kHz. The interferometer response is inversely dependent on $L(s)$, according to (5), and shows better suppression at lower frequencies—as low as -70 dB at 1 Hz. The suppression at each of these frequencies would improve with increased feedback bandwidth. At higher frequencies near the bandwidth, both responses diverge from the theory due to the emergence of higher-order dynamics in the scanner. Single point measurements at these frequencies are not representative of this complicated behaviour.

3.2. Imaging with disturbance suppression—tapping mode AFM

The disturbance suppression observed during imaging is shown in figures 5 and 6. In figure 5, a gold thin film sample, identical to that used for the high-reflectance interferometer mirror, was imaged at a scan rate of 2 Hz. The grains have approximately 20 nm of topography, which is well in excess of the noise floor of the microscope in its laboratory imaging environment. However, in a hostile imaging environment such as a microfabrication facility, this would not necessarily be the case. During the image acquisition, to simulate such an environment, we tapped on the Z stepper motor of the microscope, which is used to engage the tip and is expected to pick up significant Z disturbances. Both images were identically flattened and planefit, but were otherwise unaltered. The Z scale of the interferometer image was adjusted to match the well-calibrated actuator image, with the interferometer sensitivity used to confirm the scaling factor. As observed in figure 5, mechanically disturbing the stepper motor resulted in a dramatic distortion of the actuator image, while the interferometer image was able to maintain the clarity of the gold grains in real time over the duration of the disturbance.

Images of DNA on mica are shown in figure 6, to represent the case where topography and disturbances are comparable in magnitude. In this example, the microscope was not intentionally disturbed, but ambient disturbances coupled in from the environment and affected the image quality. Plasmid DNA (D-3404, Sigma-Aldrich, USA) was prepared at a concentration of 50 μg ml^{-1} in a buffer of 40 mM Tris-HCl and 10 mM $MgCl_2$ at pH 7.6 [8]. A few drops of the DNA solution were placed on a freshly cleaved mica substrate (SPI Supplies, USA), incubated for 10 min, rinsed in water, and blown dry. Images were acquired at a 2 Hz scan rate with 512 pixels per line. 4 out of the 400 scan lines were removed from both images due to common-mode scan artifacts, and both images were equivalently flattened and planefit. Each scan line in both images was also filtered offline with a 20th order, 500 Hz zero-phase finite impulse response filter to remove common-mode high-frequency noise. The actuator image appears streaked due to Z disturbance effects and suffers from 60 Hz diagonal background stripes. The interferometer image does not exhibit streaking and shows suppressed background noise, suggesting that some of the 60 Hz line noise may induce mechanical disturbances through the actuator or cantilever.

We do not claim that image improvement will be comparable to these results on all SPMs and in all imaging environments. At present, this technique will be most effective in very noisy environments, such as a microfabrication facility, where Z disturbances overwhelm sample topography. However, there are two significant implications of this work:

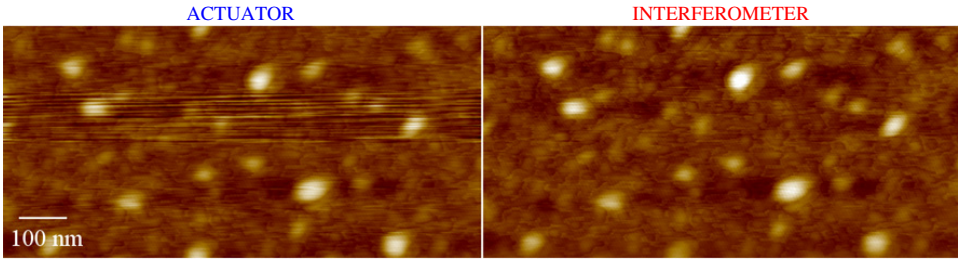

Figure 5. A gold thin film sample imaged simultaneously in air by the actuator and interferometer using tapping mode AFM. The sample was scanned at 2 Hz. The streaks are a result of physically shaking the Z stepper motor of the microscope and appear suppressed in the interferometer image. The Z scale is 20 nm.

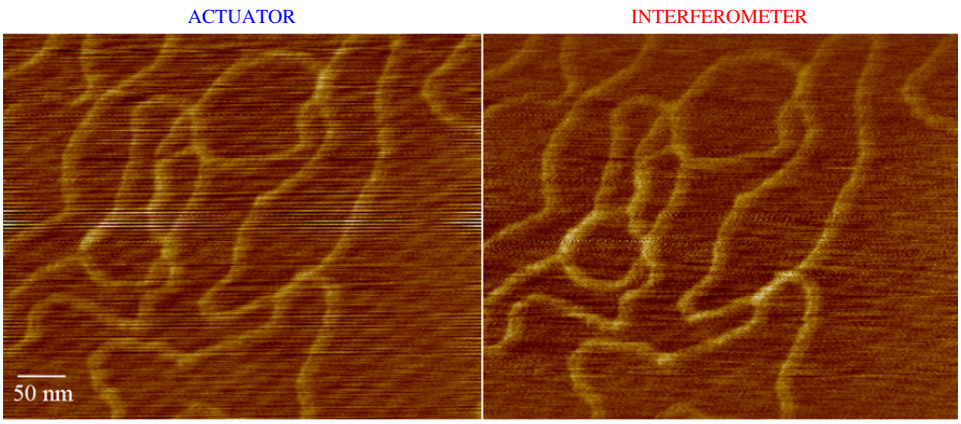

Figure 6. Tapping mode AFM images of DNA on mica in air with a 2 Hz scan rate. Ambient Z disturbances coupling into the microscope are suppressed in the interferometer image. The Z scale is 2 nm.

(1) vibration isolation, which is costly and consumes space, can be rendered unnecessary for noisy environments; and
(2) this technique can potentially outperform vibration isolation in virtually any ambient environment with further reduction of the interferometer noise floor. Interferometers with less than 0.01 nm rms in a DC to 1 kHz bandwidth have been demonstrated for AFM [5].

3.3. Limitations and outlook

A critical limitation of the disturbance suppression technique is that it is insensitive to lateral, or XY, disturbances that cannot be distinguished from topography and can be comparable in magnitude to out-of-plane disturbances. The situation is particularly problematic because the partially reflective mirror of the interferometer cannot be adjusted in this configuration so that it is perfectly aligned with the Z axis of the actuator. Therefore, the actuator actually measures a small component of lateral motions between tip and sample. In the future, we hope to incorporate diffractive structures with the interferometer that can detect lateral as well as out-of-plane motions and compensate accordingly.

The angular mismatch between the partial mirror and the Z axis also limits the scan size due to biasing issues. The interferometer output depends sinusoidally on separation [6], and biasing ensures it is operating in a linear regime on a point of maximum slope. The angular mismatch allows biasing by lateral offset of the tip on the sample, but scan sizes greater than a few microns cause the bias point to drift out of its linear range. We envision that this limitation could be eliminated by using a tunable laser or by mounting a small piezo element between the probe and interferometer, either of which could be controlled by a slow feedback loop to counteract bias point drift.

XY disturbances also prevent isolated measurements of each noise source, making it difficult to fully characterize the limitations of the microscope. Implementation on a less noisy microscope, with smaller XY disturbances, or one with effective compensation for XY disturbances would allow a more complete noise characterization and also provide an effective platform for low noise scanning probe spectroscopy. Although there are several reports of using secondary sensors to stabilize spectroscopy measurements [9, 10], our approach is unique in its ability to suppress disturbances in either scanning or spectroscopic modes. In the spectroscopic mode, using the interferometer for feedback, the fundamental measurement limit would be determined by the noise of both sensors. Equations (6) and (7) can be easily adapted to show that this is the case.

4. Conclusions

We have demonstrated an adaptation of the inherent disturbance suppression technique that allows it to be used with any scanning probe imaging or spectroscopy mode without any custom microfabricated components. An interferometer is used to measure the average separation between the sample and the base of the scanning probe over an area of the sample

that is much larger than the tip. While scanning laterally with the localized probe sensor in feedback, the delocalized interferometer output reveals topography and substantially suppresses out-of-plane disturbances for frequencies within the feedback bandwidth. This measurement is limited by lateral disturbances and noise from the scanning probe sensor and interferometer.

The technique was implemented on a disturbance-susceptible commercial microscope using a Fabry–Perot interferometer. Suppression as great as 70 dB at 1 Hz was observed. We show improvement in imaging nanostructures by using the interferometer for image construction, both with gold grains (10 nm scale) in the presence of large, synthesized disturbances and with single DNA molecules (1 nm scale) subjected to ambient disturbances. Furthermore, the separation between the two sensors allows any sample to be imaged, regardless of its ability to diffract the interferometer laser.

Acknowledgments

The authors thank Craig Prater of Veeco Instruments, Thomas Burg of MIT, and Cagri Savran of Purdue University for helpful suggestions and Nebojsa Milovic of MIT for sample preparation expertise. This work was supported by the Air Force Office of Sponsored Research (AFOSR) contract F49620-02-1-0322.

References

[1] Abraham D W, Williams C C and Wickramasinghe H K 1988 *Appl. Phys. Lett.* **53** 1503
[2] Proksch R and Dahlberg E D 1993 *J. Appl. Phys.* **73** 5808
[3] Schitter G and Stemmer A 2002 *Nanotechnology* **13** 663
[4] Sparks A W and Manalis S R 2004 *Appl. Phys. Lett.* **85** 3929
[5] Rugar D, Mamin H J and Guethner P 1989 *Appl. Phys. Lett.* **55** 2588
[6] Manalis S R, Minne S C, Atalar A and Quate C F 1996 *Appl. Phys. Lett.* **69** 3944
[7] Zhong Q, Inniss D, Kjoller K and Elings V B 1993 *Surf. Sci. Lett.* **290** L688
[8] Bezanilla M, Manne S, Laney D E, Lyubchenko Y L and Hansma H G 1995 *Langmuir* **11** 655
[9] Altmann S M, Lenne P-F and Horber J-K H 2001 *Rev. Sci. Instrum.* **72** 142
[10] Abe M, Sugimoto Y, Custance O and Morita S 2005 *Nanotechnology* **16** 3029